Journal of Machine Engineering, 2024, Vol. 24, No. 3, 106–118
ISSN 1895-7595 (Print) ISSN 2391-8071 (Online)

Received*: 08 May 2024* / Accepted: *11 June 2024* / Published online: *30 August 2024*

investment casting, surface roughness, SLA, wax pattern, 3DP mold

Thanh Tan NGUYEN[1],
Dao Hai SON[1],
Van Tron TRAN[1*]

A STUDY ON THE ABILITY TO FABRICATE MOLD USING 3D PRINTING TECHNOLOGY AND EVALUATE THE SURFACE ROUGHNESS OF PRODUCTS IN INVESTMENT CASTING

The investment casting (IC) process is a technique used to produce high-precision metal castings, including complex shapes and metals that are difficult to cast using conventional methods. Typically, the process begins by creating a wax pattern from a mold in the initial steps. The molds used for IC are fabricated using conventional machining techniques. However, this mold preparation approach can be challenging when it comes to fabricating complex shapes and thin walls, particularly in small-batch production scenarios. To overcome this limitation, this study explores a flexible design approach that utilizes three-dimensional printing (3DP) to fabricate IC molds. The key advantage of this approach is the combination of the flexible design mold and the surface roughness (SR) of the casted parts. The experimental results demonstrate that the SR of the casted products fabricated using the 3DP mold is comparable to that obtained from the conventional mold-making process. These findings provide an alternative strategy for preparing IC molds with high flexibility, which can accommodate various scales of production. The 3DP-based approach offers a more adaptable solution compared to conventional machining methods, particularly for complex geometries and small-batch manufacturing.

1. INTRODUCTION

The investment casting (IC) process, also known as the lost wax process, is a foundry technique for producing high-precision metal castings [1, 2]. One of the primary advantages of this process is its ability to create castings with a smooth surface finish, complex shapes, thin walls, and delicate features that would be challenging or impossible to machine using traditional methods [3, 4]. Moreover, IC is particularly well-suited for casting complex shapes and features that would be difficult or improbable to produce using other casting techniques, such as sand casting, squeeze casting, die casting, semi-solid die casting, and plaster mold casting, as this technique has no metallurgical limitations [5, 6]. As a result, a wide range of

[1] Faculty of Mechanical Engineering, Ho Chi Minh City University of Technology and Education, Vietnam
[*] E-mail: trontv@hcmute.edu.vn
https://doi.org/10.36897/jme/189942

products with high-quality surfaces has been produced using IC, including turbine blades, electrical equipment and electronic hardware, radar systems, statues and art castings, prosthetics, golf club heads, agricultural equipment, machine tool components, hand tools, fuel systems, jewellery, aircraft engines, turbochargers, computer hardware, automobile components, dental applications [7–9]. This versatility and ability to produce complex, high-precision castings make the IC process a valuable tool in a wide range of industries.

The molds are typically manufactured using conventional machining techniques to produce wax patterns for the investment casting (IC) process. However, this approach displays certain limitations when fabricating particular features, such as thin-wall thickness, sharp corners, undercuts, etc…. These constraints can significantly increase fabrication costs and time, especially for small-batch production [10, 11]. These disadvantages of traditional mold fabrication for IC can be overcome by utilizing additive manufacturing (AM) technology, also known as 3D printing or rapid prototyping [8, 9, 12]. This toolless manufacturing technology involves connecting materials to create objects from 3D model data, often layer by layer, as opposed to subtractive manufacturing methodologies [13, 14]. The flexibility of this approach allows for the preparation of patterns for fabricating IC molds with enhanced design flexibility, minimum energy consumption, and reduced time to market, particularly for small-batch productions and complex shapes [15–17]. According to a recent report, the lead time and production costs could be reduced by 60% and 89%, respectively, by using AM in IC [12]. Chander Prakash and co-workers demonstrated that employing AM in IC not only reduces cost and time but also energy consumption and CO2 emission [16]. Recently, 3DP technology has also been employed to prepare plastic injection molds [18–21]. For instance, the rectangular cooling channels of the 3D printed mold were developed to reduce the cycle time in plastic injection molding [18]. John Ryan C. Dizon and co-workers fabricated injection molds with different 3DP ways and materials in polymers to compare their dimensional accuracy [5, 10, 20, 22].

While there have been some reports on the use of 3D printing (3DP) in plastic injection molding, there is a lack of comprehensive studies exploring the application of 3DP in the manufacturing of investment casting (IC) molds and/or providing a transparent comparison of the efficiency between 3DP and traditional methods for preparing IC molds. To address this technological gap, this study evaluates the potential of using 3DP for fabricating IC molds. The potential applications of the developed mold in the real world are investigated in terms of the surface roughness (SR) of the casted parts, which was compared to that obtained from the traditional aluminum mold.

2. MATERIALS AND METHODS

2.1. MATERIALS

Rigid 10K resin, supplied by 3D Smart Solutions Company, Vietnam, is used for SLA (Stereolithography) 3DP. The thermal conductivity of the resin is shown in Table 1.

For comparison, 6061 aluminum (Al) is used to manufacture the IC mold. This class of Al is widely employed in wax molding since it has excellent thermal conductivity, corrosion, and low price [23]. Tables 2 and 3 show the chemical composition and the thermal conductivity of 6061 Al.

Table 1. Thermal conductivity of rigid 10K resin [23]

Temperature ◦C	Value W/(m K)
40	0.5
50	0.53
60	0.55

Table 2. Chemical composition of Al 6061 [24]

Element	Mg	Fe	Si	Cu	Mn	V	Ti	Al
Weight %	1.08	0.17	0.63	0.32	0.52	0.01	0.02	Remainder

Table 3. Thermal conductivity of Al6061 [25]

Temperature ◦C	Value W/(m.K)
50	154.9
100	158.3
150	160.1

A wax mixture of 118174 Freeman Flakes Wax—Super Pink from (Freeman Manufacturing & Supply Company, Avon, OH, United States) was used to prepare IC patterns. Its thermal conductivity is shown in Table 4 [23].

Table 4. Thermal conductivity of wax [23]

Temperature ◦C	Value W/(m.K)
40	0.35
50	0.37
60	0.39

SKD61 steel was used as a casting substance. It is supplied by the manufacturer JUKI (VIETNAM) CO., LTD. The nominal chemical composition of SKD61 steel is given in Table 5.

Table 5. Chemical composition of SKD11

Element	C	Si	Cr	Mo	V	Mn	Fe
Weight %	≤0.38	≤0.1	≤5.0	≤1.25	≤1.0	≤0.4	Remainder

2.2. METHODS

2.2.1. PREPARATIONS OF THE MOLDS

Preparation of 3DP mold cavity. First, the cavity was designed using Creo Parametric 8.0 (PTC, Boston, Massachusetts, United States). Next, the STereoLithography (STL) file was exported from the design (Fig. 1a). After that, the STL geometry file was preprocessed utilizing the slicer program Formlabs Preform (Fig. 1b). The appropriate algorithm parameters, supports, and laser pathways were selected and generated on layers for printing the designed model. The layer thickness was established at 50 μm. Next, the obtained 3D-printed cavity was washed using Formlabs Form Wash (Fig. 1c). To get rid of the liquid resin on the part surfaces, the 3D-printed cavity was immersed in high-purity 99.9% isopropyl alcohol (IPA) for 20 minutes in a Formlabs Form Wash machine (Fig. 1d). After removing all of the supports using a cutter, the cavity experienced heat treatment and UV exposure in a Formlabs Form Cure machine. The time for printing cavities, washing at room temperature, UV curing at 60°C, and heat treatment at 125°C was 722 min, 20 min, 60 min, and 90 min, respectively (Table 6). The manufacturing and assembly steps of the 3DP mold are shown in Fig. 1d.

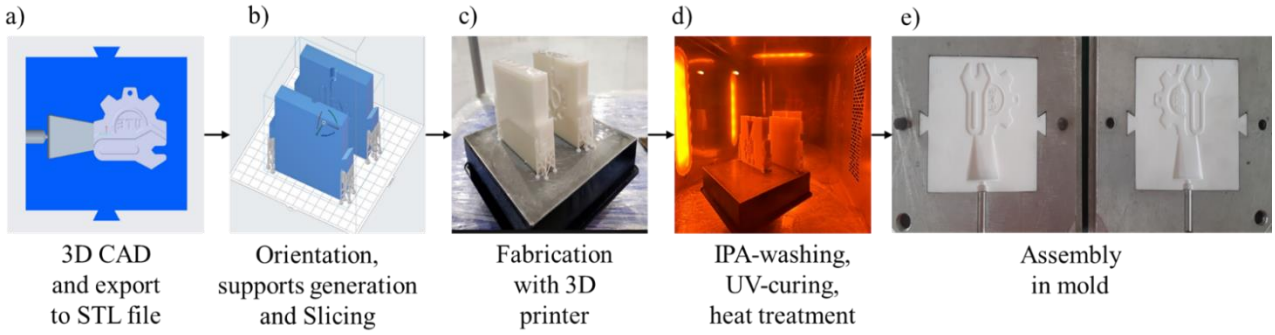

Fig. 1. Process making 3DP mold for IC

Table 6. Post-processing (washing IPA, UV, and heat treatments) used for materials

Post-Processing	Temperature (◦C)	Time (min)
Washing IPA	RT	20
UV curing	60	60
Heat treatment	125	90

Preparation of the aluminum mold. First, a CAD model of the mold was designed using Creo Parametric 8.0. The CNC machine's tool paths and G-codes were then generated using the Mastercam software (CNC Software, Tolland, Connecticut, US). Next, the CNC machine with the cutting tools was set up. Then, the 6061 Al workpiece was fabricated to obtain the mold.

2.2.2. FABRICATIONS OF THE IC PATTERNS

First, the wax is heated at 53°C. Then, it was injected into the molds, including 3DP and 6061-Al molds, by the vertical injection machine. After the cooling step, the pattern was ejected from the molds. Table 7 shows the parameters of this process.

Table 7. The parameters of the injection process

Specifications	Unit	Value
Holding time	s	5 to 30
Cooling time	s	2
Wax temperature	°C	53
Cooling temperature	°C	24
Injection pressure	MPa	30
Holding pressure	MPa	65

2.2.3. SHELL MOLD PREPARATIONS FOR IC CASTING

The shell molds were prepared following the methodology described in a previous study [26]. First, wax patterns were coated with ceramic material four times. Specifically, the patterns were dipped in a ceramic slurry composed of 16.86% colloidal silica 830, 83.3% zircon flour, 0.1% defoaming agent, and 0.06% degassing agent. After the ceramic coating, the patterns were covered in ceramic particles, including zircon 22 s and zircon 35 s. The coated patterns were then dried at 25°C and 70% humidity (as shown in Fig. 2a). Finally, to create the mold cavities, the wax patterns were extracted from the outer ceramic shell and heated to 1000°C in a furnace. These cavities were subsequently used for casting molten SKD61 alloy.

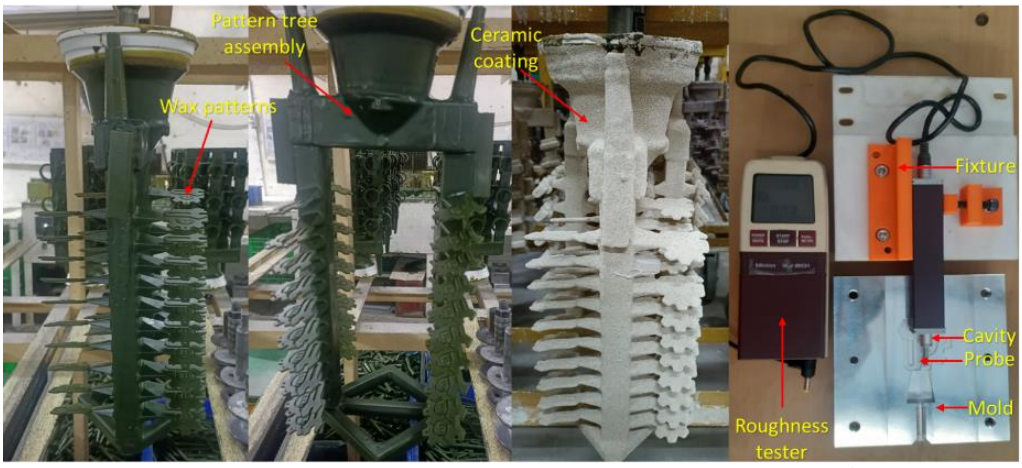

Fig. 2. (a) Shell mold preparations. (b) The surface roughness tester and a fixture

2.2.4. SURFACE ROUGHNESS MEASUREMENTS

The surface roughness of the prepared molds, cast wax patterns, and cast products was measured using a Mitutoyo SJ-210 surface roughness tester (Mitutoyo, Kawasaki, Kanagawa, Japan), as shown in Fig. 2b. The roughness parameter Ra (μm) was evaluated using a cutoff length of 0.8 mm. Various positions on the prepared molds, cast wax patterns, and cast products, which were prepared using 3DP and 6061-Al molds, were inspected to compare the surface roughness. The same measurement locations were investigated for each type of model.

3. RESULTS AND DISCUSSION

In this research, the mold cavity was 3D printed using an SLA printer and a rigid 10K resin material. This 3DP mold cavity was then assembled into a 6061 aluminum mold base, as shown in Fig. 3a(i). For comparison, a 6061-Al mold was also manufactured separately using a CNC machining process, as depicted in Fig. 3a(ii). Both the 3DP and CNC-machined molds were then installed on a vertical injection molding system, and experiments were conducted to evaluate their ability to create wax patterns (Fig. 3b). The results demonstrated that all the desired features were successfully fabricated in the wax patterns using both types of molds (Fig. 3c). These wax samples were subsequently employed to prepare the ceramic shell molds used for casting the final products (Fig. 3d).

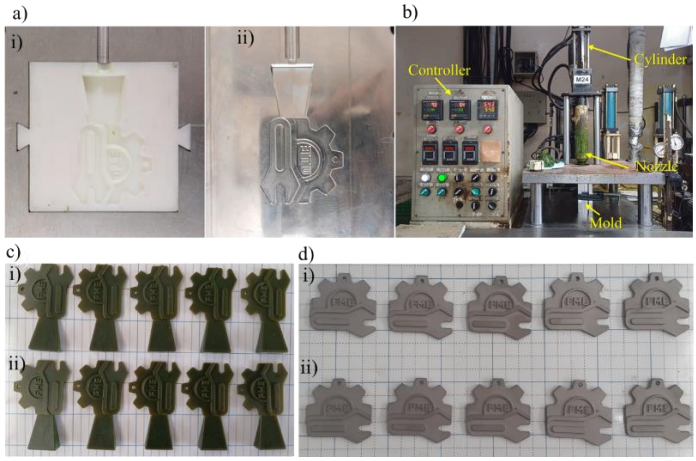

Fig. 3. (a) The molds for IC: (i) 3PD mold and (ii) 6061-Al mold. (b) The molds were mounted in a wax vertical injection molding machine. (c) The injected wax patterns: (i) wax patterns prepared from the 3PD mold and (ii) wax patterns obtained from the 6061-Al mold. (d) The IC casted parts: (i) casted parts produced using the 3PD mold and (ii) the part manufactured using the Al mold

3.1. SURFACE ROUGHNESS OF THE CAVITY

Surface roughness of the mold cavity is one of the most critical factors in investment casting, as it directly impacts the quality of the casted parts in terms of strength, weight, dimensional accuracy, porosity, microstructure, and residual stress [13, 27–29]. This section discussed the measurement and evaluation of the SR of the 3DP and 6061-Al mold cavities.

The effect of mold surface roughness on the wax patterns and casting parts is also explored in the following sections. The SR of the molds was measured at the same positions as shown in Fig. 4a,b. During the testing, the tester probe moved horizontally at positions 1, 2, 3, 4, 5, 7, 8, 9, 10, 11, and 12. At positions 6 and 12, the probe moved vertically.

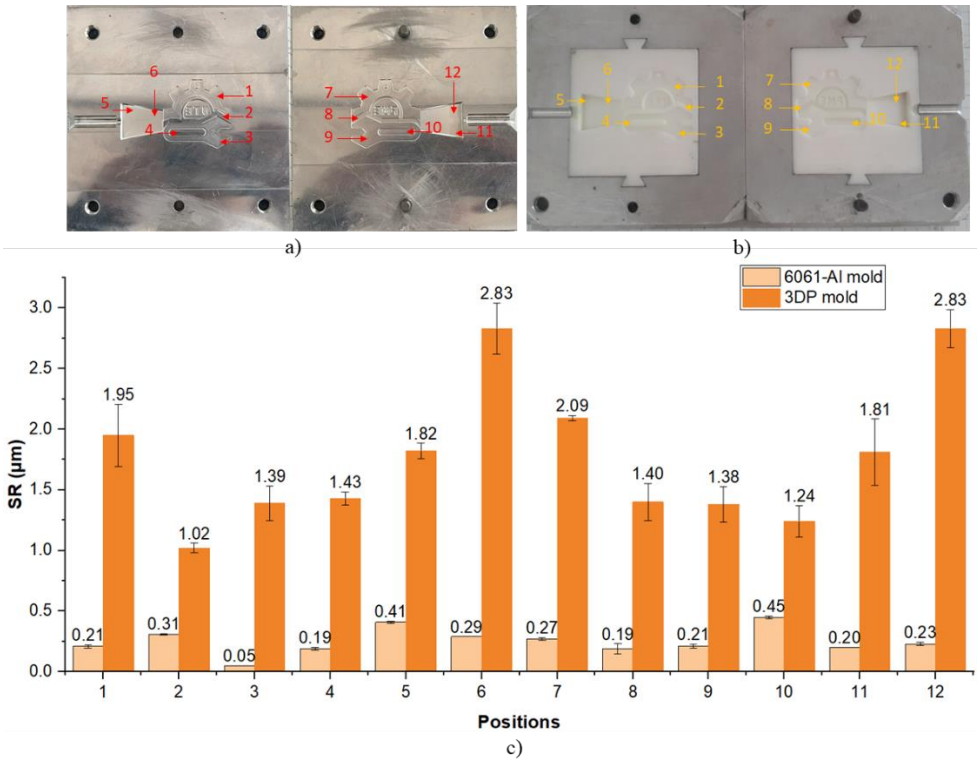

Fig. 4. The positions were measured SR of cavity mold (a) 6061-Al and (b) 3DP molds. (c) The SR values were measured at various positions in the cavities of the 6061-Al and 3DP molds. In plots (c), the error bars indicate the standard deviations (n = 3)

The SR values of the cavity in the 6061-Al mold and the 3DP mold are shown in Fig. 4c and Table 8. The results indicate that the SR of the 6061-Al mold was lower than that measured in the 3DP insert mold at all positions. The arithmetic average SR of the 6061-Al mold ranged from 0.05 µm to 0.45 µm, while the SR of the 3DP mold fluctuated between 1.02 µm and 2.83 µm. The significant variation of the obtained SR in each mold was probably due to the different moving directions of cutting tools or printing nozzles during fabrication [26, 30]. The highest SR value of 0.45 µm for the former was obtained at position 10, and the lowest value of 0.05 µm was measured at position 3. For the latter, the highest SR values of ~ 2.83 µm were observed at positions 6 and 12, while the lowest value of 1.02 µm was measured at position 8 (Fig. 4c and Table 8). The higher SR at positions 6 and 12 of the 3DP insert mold was likely because the roughness measurement direction was perpendicular to the printing direction [27]. Additionally, the SR of the 3DP insert mold was more variable than that of the 6061-Al mold, as it was also influenced by other printing parameters such as blade gap, hatch space, and position on the build platform [31]. This is because 3D printing builds parts layer by layer, resulting in inherently higher SR compared to traditional machining methods [29].

Table 8. The SR values were measured at various positions in the cavities of the 6061-Al and 3DP molds

Positions	Type of mold									
	6061-Al mold					3DP mold				
	1st	2nd	3rd	Arithmetic average	Standard deviation	1st	2nd	3rd	Arithmetic average	Standard deviation
1	0.23	0.20	0.20	0.21	0.014	2.29	1.90	1.67	1.95	0.256
2	0.31	0.30	0.31	0.31	0.006	1.08	1.00	0.99	1.02	0.040
3	0.05	0.05	0.05	0.05	0.000	1.56	1.39	1.21	1.39	0.143
4	0.19	0.18	0.21	0.19	0.013	1.38	1.40	1.50	1.43	0.053
5	0.40	0.42	0.41	0.41	0.008	1.82	1.90	1.74	1.82	0.065
6	0.29	0.29	0.29	0.29	0.000	3.11	2.78	2.60	2.83	0.211
7	0.29	0.27	0.26	0.27	0.013	2.12	2.07	2.08	2.09	0.022
8	0.14	0.2	0.24	0.19	0.041	1.54	1.48	1.19	1.40	0.153
9	0.23	0.22	0.19	0.21	0.017	1.30	1.25	1.58	1.38	0.145
10	0.44	0.46	0.46	0.45	0.01	1.10	1.20	1.41	1.24	0.129
11	0.20	0.20	0.20	0.20	0.000	2.14	1.82	1.47	1.81	0.274
12	0.21	0.23	0.24	0.23	0.013	3.03	2.82	2.65	2.83	0.155

3.2. SURFACE ROUGHNESS OF THE WAX PATTERNS

After the wax patterns were injected, the SR was measured at various positions (Fig. 5a,b) to investigate the SR of the wax patterns. The results for the wax patterns obtained from the two molds are shown in Fig. 5c and Table 9. The wax patterns produced using the 6061-Al mold (Al-patterns) had a smaller SR compared to the patterns made with the 3DP mold (3DP-patterns) at positions 1, 2, 3, 6, 8, 9, 10, and 12. However, the Al-patterns had a higher SR than the 3DP-patterns at positions 4, 5, 7, and 11. The arithmetic average SR of the 3DP-patterns ranged from 0.60 µm to 1.73 µm, while that of the Al-patterns varied between 0.61 µm and 1.64 µm. For the 3DP-patterns, the highest and lowest SR values were at positions 12 and 3, respectively, while the highest and lowest SR for the 6061-Al mold were at positions 11 and 9, respectively (Fig. 5c and Table 9).

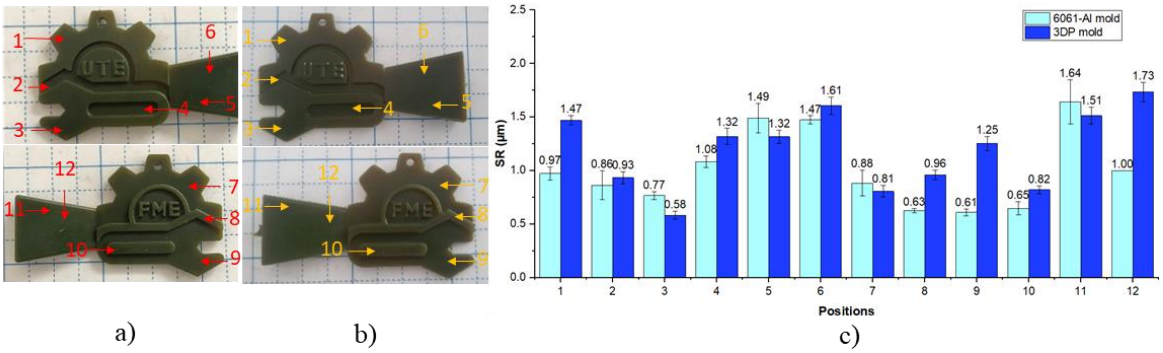

Fig. 5. The positions for measuring the SR of wax pattern form (a) Al-patterns and (b) 3DP-patterns. (c) The SR value of the Al-patterns and 3DP-patterns. In plots (c), the error bars indicate the standard deviations (n = 3)

Although the fabricated molds had different SR, the SR of the resulting wax patterns was comparable. This was likely due to the high surface tension of the molten wax, which prevented it from filling the micro slots in the printed surface during the wax injection process [30]. The reduction in SR from the molds to the wax patterns achieved in this research was much greater than in previous studies. For example, the SR of FDM-based ABS patterns was reduced from 21.63 to 14.40 μm with pre-processing treatments [32], and the printed part surface could be improved to reach Ra = 3.2 μm [33]. The SR of the wax patterns in this study was similar to the 0.8–2.4 μm range reported in recent related studies [34, 35].

Table 9. SR value of a wax pattern made from the 3DP and 6061-Al molds

Positions	Wax pattern from									
	6061-Al mold					3DP mold				
	1st	2nd	3rd	Arithmetic average	Standard deviation	1st	2nd	3rd	Arithmetic average	Standard deviation
1	1.05	0.97	0.90	0.97	0.061	1.46	1.53	1.42	1.47	0.045
2	1.00	0.91	0.68	0.86	0.135	0.94	1.00	0.86	0.93	0.057
3	0.82	0.74	0.74	0.77	0.038	0.53	0.61	0.61	0.58	0.038
4	1.04	1.16	1.05	1.08	0.054	1.24	1.3	1.42	1.32	0.075
5	1.35	1.44	1.68	1.49	0.139	1.36	1.36	1.23	1.32	0.061
6	1.42	1.49	1.51	1.47	0.039	1.60	1.51	1.71	1.61	0.082
7	1.05	0.84	0.76	0.88	0.122	0.79	0.88	0.75	0.81	0.054
8	0.6	0.64	0.64	0.63	0.019	1.00	0.98	0.90	0.96	0.043
9	0.65	0.61	0.57	0.61	0.033	1.18	1.24	1.34	1.25	0.066
10	0.58	0.73	0.63	0.65	0.062	0.77	0.85	0.84	0.82	0.036
11	1.43	1.58	1.92	1.64	0.205	1.62	1.43	1.49	1.51	0.079
12	1.00	1.00	1.00	1.00	0.000	1.84	1.62	1.74	1.73	0.090

3.3. SURFACE ROUGHNESS OF THE CASTED PARTS

The casted parts fabricated using the 3DP-patterns and Al-patterns are referred to as 3DP-casted and Al-casted parts, respectively. Their SR was measured at various positions, as shown in Figures 6a,b. During testing, the probe of the measurement device moved horizontally across all positions. Compared to other recent studies, the SR of the cast parts obtained in this research was much lower than that of metal castings made from ice patterns and wax patterns [36–38]. The SR of the 3DP-casted parts was comparable to that of the Al-casted parts at most positions (Fig. 6c and Table 10). The arithmetic average SR ranged from 2.26 μm to 3.57 μm for the 3DP-casted parts and 2.29 μm to 3.85 μm for the Al-casted parts. At positions 1, 3, and 9, the SR of the two types of cast parts was similar. The highest SR was located at position 8 for both types of cast parts. Despite the big differences in SR between the two types of molds, the SR of the final cast parts was comparable. This result clearly indicates that the lower quality in SR of the molds prepared by the 3DP technique could still produce IC-casted parts with high-quality surface finish. This phenomenon was most likely caused by the high surface tension of the molten metal, which hindered it from completely

filling the micro slots in the printed mold surface during casting [26, 27, 39, 40]. Surprisingly, the SR of the 3DP-casted parts obtained in this research was much lower than that of the metal castings made from ice patterns and wax patterns in other recent studies [36–38], even matching the quality of wax-coated parts [41].

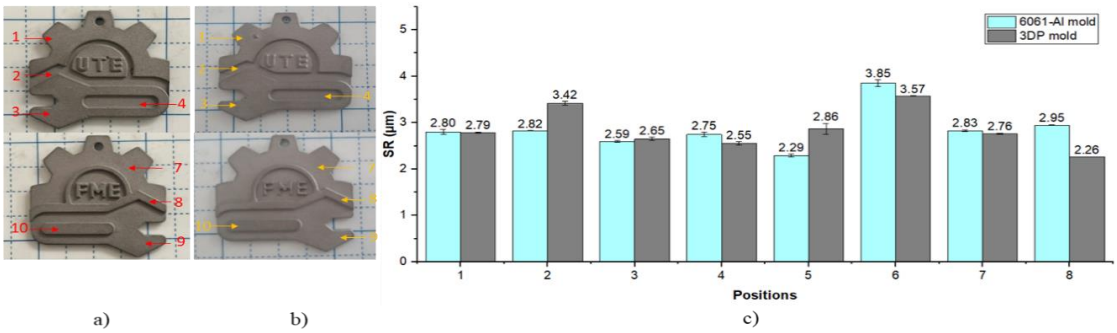

Fig. 6. The positions for measuring the SR of (a) Al-casted parts and (b) 3DP-casted parts. (c) The SR value of the Al-casted parts and 3DP-casted parts. In plots (c), the error bars indicate the standard deviations (n = 3)

Table 10. The SR of casted parts

Positions	The SR of casted parts using									
	6061-Al mold					3DP mold				
	1	2	3	Arithmetic average	Standard deviation	1	2	3	Arithmetic average	Standard deviation
1	2.77	2.88	2.75	2.80	0.057	2.80	2.77	2.79	2.79	0.012
2	2.82	2.82	2.83	2.82	0.005	3.37	3.47	3.41	3.42	0.041
3	2.58	2.58	2.62	2.59	0.019	2.60	2.67	2.68	2.65	0.036
4	2.72	2.71	2.81	2.75	0.045	2.60	2.54	2.52	2.55	0.034
7	2.33	2.29	2.25	2.29	0.033	2.70	2.93	2.96	2.86	0.116
8	3.81	3.79	3.95	3.85	0.071	3.58	3.57	3.57	3.57	0.005
9	2.83	2.8	2.85	2.83	0.021	2.78	2.75	2.76	2.76	0.012
10	2.96	2.94	2.94	2.95	0.009	2.27	2.26	2.26	2.26	0.005

4. CONCLUSIONS

This study evaluated the feasibility of applying 3DP technology in IC. Both 3DP and 6061-Al molds were first manufactured and then used to fabricate IC-wax patterns and IC-casted parts. The SR of the fabricated molds, wax patterns, and cast parts were inspected at various positions. For comparison, the SR was measured at the same locations for each type of component, and the obtained arithmetic average values are as follows:

- The SR of the 6061-Al mold ranged from 0.05 µm to 0.45 µm, while the 3DP mold varied from 1.02 µm to 2.83 µm.
- The SR of the Al-wax patterns, made using the 6061-Al mold, ranged from 0.61 µm to 1.64 µm. The SR of the 3DP-wax patterns produced from the 3DP mold was 0.60 µm to 1.73 µm.

- The SR of the Al-cast parts, manufactured using the Al-wax patterns, ranged from 2.29 μm to 3.85 μm. The SR of the 3DP-cast parts, made using the 3DP-wax patterns, varied from 2.26 μm to 3.57 μm.

The results indicate that even though the IC mold fabricated by the 3DP technique had a higher SR than the mold made by conventional CNC machining, the final IC-casted SKD61 products prepared using these molds had similar surface quality in terms of surface roughness. These findings strongly support using 3DP technology in IC for small-batch production to fabricate complex shapes, flexible designs, and thin-walled parts.

ACKNOWLEDGEMENTS

We would like to express our deep gratitude to Ho Chi Minh City University of Technology and Education and Material Testing Laboratory for sponsoring the machines and equipment for the experiment. We express our gratitude to 3DS Smart Solutions Co., Ltd. for providing the 3D printer used to create molds. Additionally, we would like to thank the reviewers and editors for their constructive comments and suggestions for improving our work.

REFERENCES

[1] DEJENE N.D., LEMU H.G., GUTEMA E.M., 2023, *Critical Review of Comparative Study of Selective Laser Melting and Investment Casting for Thin-Walled Parts*, Materials, 16/23, Multidisciplinary Digital Publishing Institute (MDPI), Dec. 01, 2023, https://doi.org/10.3390/ma16237346.

[2] LIU C., JIN S., LAI X., WANG Y., 2015, *Dimensional Variation Stream Modeling of Investment Casting Process Based on State Space Method*, Proc. Inst. Mech. Eng. B. J. Eng. Manuf., 229/3, 463–474, https://doi.org/10.1177/0954405414530900.

[3] SINGH S., SINGH R., 2016, *Precision Investment Casting: A State of Art Review and Future Trends*, Proceedings of the Institution of Mechanical Engineers, Part B: Journal of Engineering Manufacture, 230/12. SAGE Publications Ltd, 2143–2164, https://doi.org/10.1177/0954405415597844.

[4] LUMLEY R.N., 2018, *Aluminium Investment Casting and Rapid Prototyping for Aerospace Applications*, Fundamentals of Aluminium Metallurgy, Elsevier, 123–158, https://doi.org/10.1016/b978-0-08-102063-0.00004-7.

[5] VYAS A., MUSHRIFF O., ROCHANI A., DOSHI T., GUPTA S., SUTARIA M., 2021, *Rapid Tooling in Investment Casting: Investigation on Surface Finish of Mould Produced with 3D Printed Patterns*, in AIP Conference Proceedings, American Institute of Physics Inc., https://doi.org/10.1063/5.0036171.

[6] KUMAR S., KARUNAKAR D.B., *Characterization and Properties of Ceramic Shells in Investment Casting Process*, International Journal of Metalcasting, 15/1, 98–107, https://doi.org/10.1007/s40962-020-00421-6.

[7] SINGH D., SINGH R., BOPARAI K.S., 2017, *Development and Surface Improvement of FDM Pattern Based Investment Casting of Biomedical Implants: A State of Art Review*, Journal of Manufacturing Processes, 31, https://doi.org/10.1016/j.jmapro.2017.10.026.

[8] MUKHANGALIYEVA A., DAIRABAYEVA D., PERVEEN A., TALAMONA D., 2023, *Optimization of Dimensional Accuracy and Surface Roughness of SLA Patterns and SLA-Based IC Components*, Polymers (Basel), 15/20, https://doi.org/10.3390/polym15204038.

[9] MUKHTARKHANOV M., PERVEEN A., TALAMONA D., 2020, *Application of Stereolithography Based 3D Printing Technology in Investment Casting*, Micromachines, 11/10, https://doi.org/10.3390/mi11100946.

[10] RIPETSKIY A.V., KHOTINA G.K., ARKHIPOVA O.V., 2023, *The Role of Additive Manufacturing in the Investment Casting Process*, E3S Web of Conferences, EDP Sciences, https://doi.org/10.1051/e3sconf/202341304015.

[11] RAHMATI S., REZAEI M.R., AKBARI J., 2009, *Design and Manufacture of a Wax Injection Tool for Investment Casting Using Rapid Tooling*, Tsinghua Sci. Technol., 14/1, 108–115, https://doi.org/10.1016/S1007-0214(09)70076-8.

[12] WANG J., SAMA S.R., LYNCH P.C., MANOGHARAN G., 2019, *Design and Topology Optimization of 3D-Printed Wax Patterns for Rapid Investment Casting*, Elsevier B.V, 683–694. https://doi.org/10.1016/j.promfg.2019.06.224.

[13] PATTNAIK S., *Investigation on Controlling The Process Parameters for Improving the Quality of Investment Cast Parts*, Journal of the Brazilian Society of Mechanical Sciences and Engineering, 40/6, https://doi.org/10.1007/s40430-018-1246-x.
[14] TRAN V.T., NGUYEN T.C., NGUYEN T.T., NGUYEN H.N., 2023, *Environmentally Friendly Plastic Boats – A Facile Strategy for Cleaning Oil Spills on Water with Excellent Efficiency*, Environmental Science and Pollution Research, 30, 68848–68862, https://doi.org/10.1007/s11356-023-26978-3.
[15] DUDA T., RAGHAVAN L.V., 2016, *3D Metal Printing Technology*, IFAC-PapersOnLine, Elsevier B.V., 103–110, http://doi:10.1016/j.ifacol.2016.11.111.
[16] PRAKASH C., SINGH S., KOPPERI H., RAMAKRIHNA S., MOHAN S.V., 2021, *Comparative Job Production Based Life Cycle Assessment of Conventional and Additive Manufacturing Assisted Investment Casting of Aluminium: A Case Study*, J. Clean Prod., 289, https://doi.org/10.1016/j.jclepro.2020.125164.
[17] KANG J.W., MA Q.X., 2017, *The Role and Impact of 3D Printing Technologies in Casting*, China Foundry, 143, 157–168, https://doi.org/10.1007/s41230-017-6109-z.
[18] DIZON J.R.C., VALINO A.D., SOUZA L.R., ESPERA A.H., CHEN Q., ADVINCULA R.C., 2019, *Three-Dimensional-Printed Molds and Materials for Injection Molding and Rapid Tooling Applications*, MRS Communications, 9/4. Cambridge University Press, 1267–1283, https://doi.org/10.1557/mrc.2019.147.
[19] JAHAN S.A. EL-MOUNAYRI H., 2016, *Optimal Conformal Cooling Channels in 3D Printed Dies for Plastic Injection Molding*, in Procedia Manufacturing, Elsevier B.V., 888–900, https://doi.org/10.1016/j.promfg.2016.08.076.
[20] DIZON J.R.C., VALINO A.D., SOUZA L.R., ESPERA A.H., CHEN Q., ADVINCULA R.C., 2020, *3D Printed Injection Molds Using Various 3D Printing Technologies*, Materials Science Forum, Trans Tech Publications Ltd, 150–156, https://doi.org/10.4028/www.scientific.net/MSF.1005.150.
[21] ETESAMI F., MULLENS C.D., SAHLI R.G., WEBB T.J., 2019, *Improving the Performance of 3D Printed Molds for Plastic Injection Molding*, EPiC Series in Computing, 58, 438–443.
[22] SIGIRISETTY M., 2022, *Role of Additive Manufacturing in Investment Casting Process*, Int. J. Res. Appl. Sci. Eng. Technol., 10/4, 278–286, https://doi.org/10.22214/ijraset.2022.41227.
[23] BURLAGA B., KROMA A., POSZWA P., KŁOSOWIAK R., POPIELARSKI P., STRĘK T., 2022, *Heat Transfer Analysis of 3D Printed Wax Injection Mold Used in Investment Casting*, Materials, 15/19, https://doi.org/10.3390/ma15196545.
[24] CHRISTY T.V., MURUGAN N., KUMAR S., 2010, *A Comparative Study on the Microstructures and Mechanical Properties of Al 6061 Alloy and the MMC Al 6061/TiB_2/12$_P$*, Journal of Minerals and Materials Characterization and Engineering, 9/1, https://doi.org/10.4236/jmmce.2010.91005.
[25] KUMAR R., SHRINGI D., BAIRWA K.N., 2021, *Numerical Validation of Thermal Conductivity of Al6061 Based Hybrid Nano Metal Matrix Composite Filled with Nanoparticles of Ni and Cr*, Mater Res Express, 8/11, Nov. https://doi.org/10.1088/2053-1591/ac3692.
[26] NGUYEN T.T. et al., 2023, *Influences of Material Selection, Infill Ratio, and Layer Height in the 3D Printing Cavity Process on the Surface Roughness of Printed Patterns and Casted Products in Investment Casting*, Micromachines (Basel), 14/2, https://doi.org/10.3390/mi14020395.
[27] FEDOROV K., RAVINDRAN C., FAYAZBAKHSH K., 2023, *Effects of Process Parameters on Friability and Surface Quality in the Rapid Investment Casting Process*, International Journal of Advanced Manufacturing Technology, 125/1–2, https://doi.org/10.1007/s00170-022-10777-0.
[28] SATA A., RAVI B., 2019, *Foundry Data Analytics to Identify Critical Parameters Affecting Quality of Investment Castings*, ASCE-ASME Journal of Risk and Uncertainty in Engineering Systems, Part B: Mechanical Engineering, 5/1, 2019, https://doi.org/10.1115/1.4041296.
[29] DEJENE N.D., LEMU H.G., GUTEMA E.M., 2023, *Critical Review of Comparative Study of Selective Laser Melting and Investment Casting for Thin-Walled Parts*, Materials, 16/23, https://doi.org/10.3390/ma16237346.
[30] GOLOGLU C., SAKARYA N., 2008, *The Effects of Cutter Path Strategies on Surface Roughness of Pocket Milling of 1.2738 Steel Based on Taguchi Method*, Journal of materials processing technology, 206, 7–15, https://doi.org/ 10.1016/j.jmatprotec.2007.11.300.
[31] UNKOVSKIY A., BUI P.H.B., SCHILLE C., GEIS-GERSTORFER J., HUETTIG F., SPINTZYK S., 2018, *Objects Build Orientation, Positioning, and Curing Influence Dimensional Accuracy and Flexural Properties of Stereolithographically Printed Res*in, Dental Materials, 34/12, e324–e333, https://doi.org/10.1016/j.dental.2018.09.011.
[32] TIWARY V.K., ARUNKUMAR P., DESHPANDE A.S., RANGASWAMY N., 2019, *Surface Enhancement of FDM Patterns to Be Used in Rapid Investment Casting for Making Medical Implants*, Rapid Prot. J, 25/5, https://doi.org/10.1108/RPJ-07-2018-0176.

[33] MUKHTARKHANOV M., SHEHAB E., ALI MD.H., 2022, *Process Parameter Optimization for 3D Printed Investment Casting Wax Pattern and its Post-Processing Technique*, Applied Sciences, 12/14, https://doi.org/10.3390/app12146847.
[34] BEMBLAGE O., KARUNAKAR D.B., 2011, *A Study on the Blended Wax Patterns In Investment Casting Process*, Proceedings of the World Congress on Engineering, 1, WCE 2011, July 6 - 8, 2011, London, U.K.
[35] BURMASTER D., KAINER A., LU Y., 2023, *Effects of Surface Roughness on Wax Deposition*, Geoenergy Science and Engineering, 231, A, 212383.
[36] LIU Q., LEU M.C., RICHARDS V.L., SCHMITT S.M., 2004, *Dimensional Accuracy and Surface Roughness of Rapid Freeze Prototyping Ice Patterns and Investment Casting Metal Parts*, International Journal of Advanced Manufacturing Technology, 24/7–8, https://doi.org/10.1007/s00170-003-1635-9.
[37] FEDOROV K., FAYAZBAKHSH K., RAVINDRAN C., 2022, *Surface Roughness and Dimensional Tolerances in A319 Alloy Samples Produced by Rapid Investment Casting Process Based on Fused Filament Fabrication*, International Journal of Advanced Manufacturing Technology, 119/7–8, https://doi.org/10.1007/s00170-021-08644-5.
[38] LI H., GUO Y., SHUHUI T., JIAN L., IDRISS A.I.B., 2022, *Study on Selective Laser Sintering Process and Investment Casting of Rice Husk/ Co-Polyamide (Co-PA Hotmelt Adhesive) Composite*, Journal of Thermoplastic Composite Materials, 36/6, 2311–2331, https://doi.org/10.1177/08927057221092323.
[39] LEE K., BLACKBURN S., WELCH S.T., 2015, *Adhesion Tension Force Between Mould and Pattern Wax in Investment Castings*, J. Mater. Process. Technol., 225, https://doi.org/10.1016/j.jmatprotec.2015.06.014.
[40] VYAS A.V., PANDYA M.P., SUTARIA M.P., 2020, *Effect of Mixing Proportion and Mixing Time on Primary Slurry Retention and Surface Roughness of Investment Casting Shells*, IOP Conference Series: Materials Science and Engineering, https://doi.org/10.1088/1757-899X/872/1/012094.
[41] KUMAR, P., AHUJA, I.S., SINGH, R., 2020, *Effect of Process Parameters on Surface Roughness of Hybrid Investment Casting*, Prog. Addit. Manuf., 5, 419, https://doi.org/10.1007/s40964-020-00132-8.